OBTAINMENT OF HIGH-QUALITY METALLIC EFFECTS BY USE OF SYNTHETIC PIGMENTS

J. Pérez, S. Reverter, E. Navarro

Color Esmalt (EUROARCE), l' Alcora, Castellón, Spain

ABSTRACT

Traditionally, the metallic effect found in ceramic products has always been associated with low quality in the end product. This low quality of the metallic glazes has been explained, in both the manufacturing process and the end product, as due to these being very complex and special products.

This study has sought to address the manufacture of metallic effects as a whole, taking into account factors relating to production and to the finished product. Thus, fundamental aspects have been improved, such as chemical resistance and the glaze-body fit, and a product range has been obtained that allows ceramic application under optimum conditions and improves the properties of the resulting ceramic tiles in regard to chemical resistance and fit to different ceramic bodies.

1. INTRODUCTION

The present study is based on a long process of research during which fundamental aspects have been tackled for the manufacture of ceramic tiles with a metallic appearance, in order to assure correct manufacture, such as the production process variables which previously largely conditioned their use. This preliminary work led to the development of a range of synthetic glazes based on metallic pigments (patent no. ES 2 246 166 B2), which provided the following fundamental advantages:

- Improvement of application conditions. It is known that the use of natural oxide has always led to the obtainment of glaze suspensions with terrible rheological conditions, which became an authentic martyrdom for technicians in ceramic tile production plants, and caused numerous application defects. The use of metallic pigment of a synthetic type allowed development of glaze suspensions with excellent rheological behaviour.
- Quality in the finished piece. The use of synthetic pigments facilitates the chemical reactions in the ceramic firing stage, improving to a large extent average first quality product, owing to the important decrease in firing defects.
- Cleaning. Metallised products made using synthetic pigments enormously facilitate handling because, since all types of pigmenting oxides are avoided, they do away with serious cleaning problems throughout the glaze manufacturing process (mills, sieves, tanks), and the ceramic production process in the glazing lines.

However, a series of problems remained to be solved, which have been addressed in the present study:

- Chemical resistance. During the preliminary development phase, chemical resistance was substantially improved, but optimum results were not fully reached, mainly in the tests with strong acids and alkalis. In that phase we went from the primitive glazes that obtained the worse ratings like GLC, to formulations with maximum ratings of GHB. In this project, with the support of the analytical techniques detailed below, the chemical composition of the glazes has been improved to ratings of GHA resistance to acid and alkali attack.
- Fit with the body. During the research process the fit with the body had considerably improved, owing to the reduction in the glaze coefficients of expansion, which went from a range of 140–180 to levels of 110–130, though the were still excessive and even made it necessary to use corrective backgrounds, which can always leave residual stresses in the tile and, hence, crazing and undesired curvatures. In the present development, the thermal expansion of the metallised glazes has been studied, and products have been developed with a coefficient of expansion within the normal range of ceramic bodies, which allows the obtainment of tiles fully coated with a metallised glaze, including porous tiles, avoiding the very serious problems of curvature and crazing.

The present work has led to a new metallic product range that enables ceramic effects with good technical properties to be obtained by a clean and stable manufacturing process.

2. OBJECTIVE

The purpose of this study has been to improve the chemical resistance and ceramic fit of a glaze with a metallised appearance for use in different ceramic technologies, ranging from fast double firing to porcelain tile manufacture, by the development of glaze compositions prepared from special frits and synthetic pigments. The starting metallised glaze was based on a P-Al-Fe system.[1]

3. EXPERIMENTAL

The different frits tested were obtained by fusing the raw materials in an electric furnace at a peak temperature of 1550ºC and a residence time of 30 minutes at this temperature. The frit was obtained by pouring the melt into water at ambient temperature. The glazes were prepared from frits, metallic pigments, and other crystalline raw materials by wet milling, using the necessary additives for correct application.

The glazes were characterised by Dilatometry and Optical hot stage microscopy with a MISURA instrument in order to determine the appropriate fit with the ceramic bodies.

The glazes were applied, according to their formulation, on to an unfired porous single-fire white tile body or a green porcelain tile body. The glazed pieces were fired in a roller kiln at a peak temperature of 1190ºC in the case of the porcelain tile and of 1130ºC in the case of the porous single-fired tile. Gloss was determined by a reflectometer, with angles of incidence of 20°, 60º, and 85º.

The chemical resistance of the glazed pieces was determined according to standard UNE-EN ISO 10545-13. The test time was four days, and the test reagents were strong acids and alkalis: hydrochloric acid (18% v/v) and potassium hydroxide (100g/l). The attack was classified according to the method described in this standard. With a view to establishing a quantitative criterion that would allow optimisation of the formulations, the impairment of appearance on exposure to chemical attack $\Delta\Psi$ was defined according to Equation 1:

$$\Delta\psi = \sqrt{(\Delta E_q)^2 + (\Delta\Theta)^2}$$

Equation 1

where ΔE_q is the colorimetric difference[2] between the attacked area and the initial area, and $\Delta\Theta$ is the corresponding difference in gloss for the different angles between both areas, defined according to Equation 2:

$$\Delta\Theta = \sqrt{(\Delta\Theta_{20})^2 + (\Delta\Theta_{60})^2 + (\Delta\Theta_{85})^2}$$

Equation 2

In addition, the surface and profile of the pieces subjected to attack were observed by different analytical techniques, with a view to determining the nature of the attack and the most sensitive areas of the glaze. This glaze characterisation was conducted at

I.T.C. (Instituto de Tecnología Cerámica, Castellón) for which the following techniques were used:

- Optical microscopy, up to 50x, to observe the surface of the glazes and the different crystalline species present.
- Scanning electron microscopy (SEM), for microstructural characterisation of the glazes by observation of the surface and of glaze cross-sections, with glaze analysis using an energy-dispersive X-ray analysis (EDX) instrument connected to the microscope. The observations were conducted at two different voltages: 10 kV and 20 kV. This allowed differentiation between the surface phases and those inside the sample, since the smaller the voltage, the more superficial is the signal.
- X-ray diffraction (XRD) for identification of the crystalline structures present in the glazes. For this, glaze test pieces were prepared that were fired at the working temperatures of each glaze, using the same thermal cycle that was used to obtain the glazed pieces.
- X-ray photoelectron spectroscopy (XPS) was performed with a Specs Sage 150 instrument. This technique provides both elementary information and information on the structure of the material surface bonds. The instrument has an argon ion source that allows the sample to be progressive treated by *sputtering*, and therefore, enables determination of the composition with depth. The processing rate is about 4.7 nm/min, with a sputtered area of 3x3 mm. The XPS spectra were evaluated using CasaXPS data processing software.

4. CHARACTERISTICS OF THE STARTING METALLISED GLAZES

An initial development was carried out based on two metallic glazes: a glossy porcelain glaze, Rp, and a satin glaze for porous single firing, Rm. This was done by design of experiments, using the coefficient of expansion and impairment of appearance as optimisation parameters, and the oxide chemical composition as a variable. The improved glazes Ap and Am were thus obtained. Table 1 gives the gloss data of the obtained pieces, and the coefficients of expansion of the glazes and bodies used, where the reduction in the expansion coefficients can be observed.

Reference	$\alpha_{50-300}\cdot 10^7$ (°C^{-1})	Gloss 20°	Gloss 60°	Gloss 85°	Softening T. (°C)
Porcelain tile body (**Sp**)	69.9				
Porcelain tile glaze (**Rp**)	158.0	93	158	68	1200
Porcelain tile glaze (**Ap**)	136.8	95	179	60	1170
Single-fire body (**Sm**)	63.7				
Single-fire glaze(**Rm**)	151.0	26	76	48	1020
Single-fire glaze (**Am**)	123.6	34	103	65	1030

Table 1. Fit and gloss parameters of the initial metallic glazes

Table 2 presents the results obtained when glaze **Ap** was subjected to the test for determining its chemical resistance to high concentrations of acids and alkalis. According to the classification, the main deterioration occurs when the glaze is subjected to alkali attack. If the results are compared with those of the previous glaze **Rp**, the difference is notable, as the table shows, when the differences obtained for gloss and colour between the attacked areas and the initial areas are compared. However the classification according to the standard is still not optimum.

Glaze	Reagents	Classification	ΔE	ΔΘ	ΔΨ
Rp	Hydrochloric acid 18%	GHC	3.22	29.9	30.1
	Potassium hydroxide 100 g/l	GHC	32.9	94.7	100.3
Ap	Hydrochloric acid 18%	GHB	0.34	4.97	4.98
	Potassium hydroxide 100 g/l	GHC	7.79	35.5	36.3

Table 2. Chemical resistance of glaze Ep.

It is fundamental, therefore, to understand the chemical attack mechanisms that the glazes undergo and their microscopic nature in order to be able to optimise the chemical resistance of the metallised pieces. The porcelain tile glaze **Ap** was studied, therefore, by optical and electron microscopy at 10 kV and 20 kV.

Figure 1 displays the surface of glaze **Ap** observed by optical microscopy, in which at least five phases can be distinguished: a glassy phase of a reddish brown colour, owing to the dissolved iron **(1)**, some orange areas consisting of accumulations of very small spheres **(2)**, groups of acicular crystals, always in the brown glass area **(3)**, isolated crystals, silver-coloured and very glossy **(4)** and isolated orange-coloured crystals with dendritic shapes **(5)**.

Figure 2 displays the surface of the glaze observed by electron microscopy at 20 kV. It shows the existence of the phases mentioned before: A smooth area, corresponding to the brown glass **(1)**, the orange veins formed by spheres of about 10 nm in size corresponding to phase separation in the glaze **(2)**, the accumulations of acicular crystals with a high iron content **(3)**, only observable at 20 kV, which is why they are immersed in the glaze; isolated very glossy crystals forming 6-pointed stars, which are also immersed **(4)** and the surface dendritic crystals, which contain a lighter-coloured core that only appears at 20 kV.

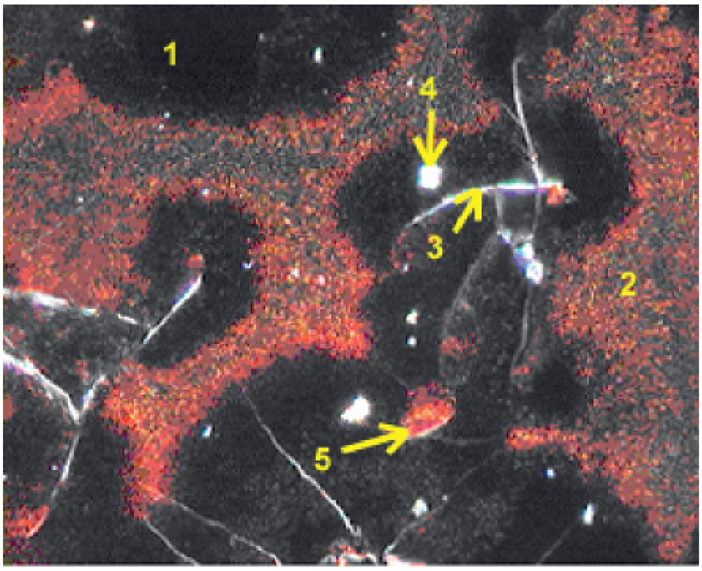

Figure 1. Surface of glaze Ap by optical microscopy

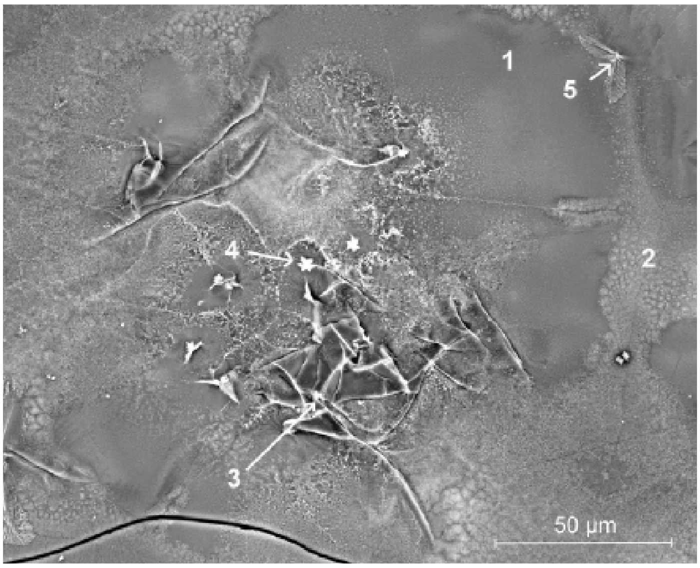

Figure 2. Surface of the glaze Ap

Figure 3 presents a detail of the phase separation area and the crazing suffered by the glaze due to the stress with the body. Figure 4 shows a cross-sectional cut of the glaze, in which four perfectly differentiated areas can be observed. The surface area **a**, consisting of a practically continuous film, of a white colour, and thickness smaller than 50 nm. A glass with a dark shade **b** and practically constant thickness of about 1 μm. An internal glaze area **d** with phase separation and an interphase area in the two previous layers **c**, formed by coalescence of drops originating in the innermost area.

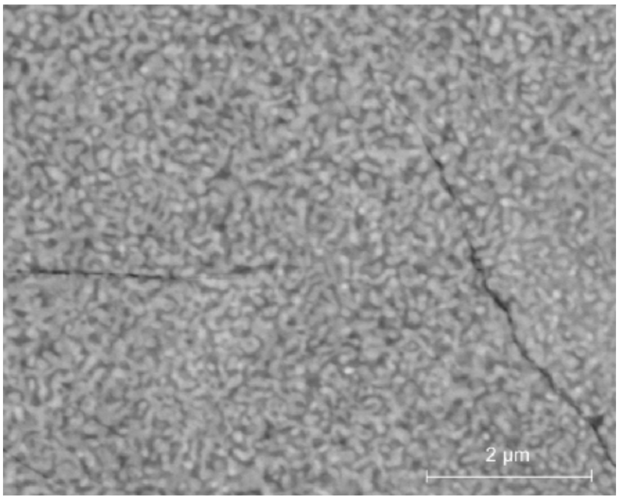

Figure 3. Detail of the surface of glaze Ap

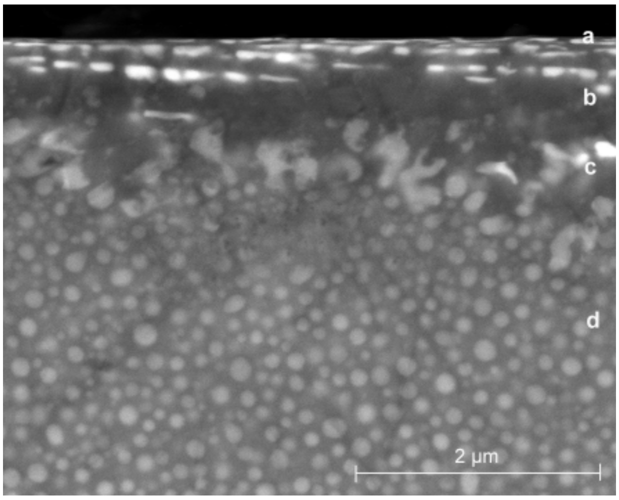

Figure 4. Detail of the cross-section of glaze Ap

With a view to obtaining more information on the different glaze layers and the effects caused in them by chemical attack, X-ray photoelectron spectroscopy (XPS) tests were conducted. Figure 5 presents the overall XPS analysis of the glaze surface, in which the high iron and oxygen content and the low phosphorus and silicon content stand out.

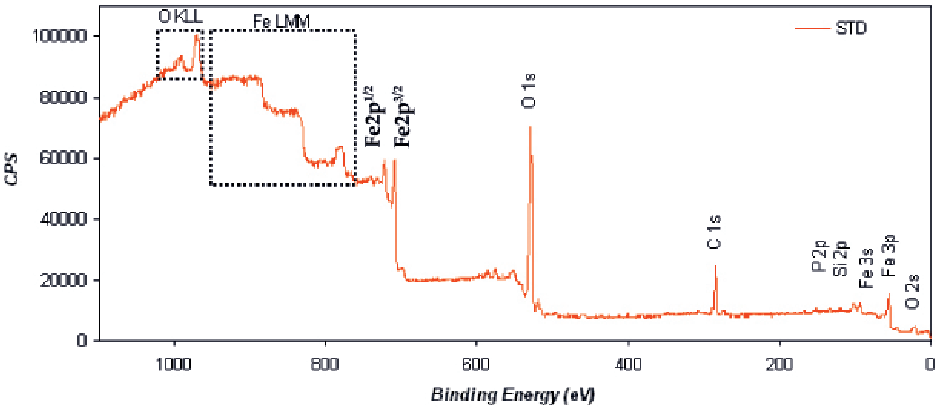

Figure 5. Overall XPS analysis of glaze Ap surface

In-depth analyses were also conducted by XPS, by progressive *sputtering*[3] with argon, which thus provided an elemental composition profile. Figure 6 presents this elemental profile, expressed in per cent, in which the quantity of oxygen has been excluded (subtracted from the sum of the percentages up to 100 %), in order to have an extended percentage scale, that would allow better observation of the variations. The figure displays four areas of different composition, marked a to d, which in a certain measure can be related to the layers identified in the SEM cross-section micrograph. As may be observed, the first layer a is almost exclusively made up of oxygen and iron. Then there is an area b with a concentration gradient mainly of iron and silicon. Farther down there are then two areas with quite stable compositions but with different iron concentrations, which could correspond to the coalescence regions c and the phase separation regions d observed by SEM.

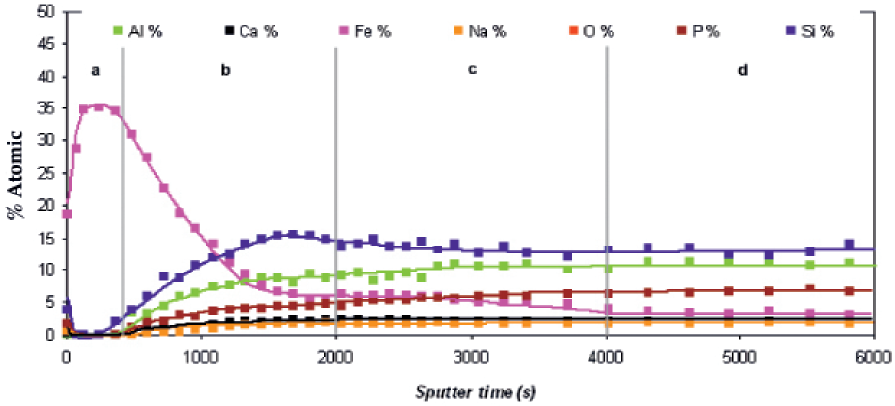

Figure 6. In-depth composition profile of sample Ap (excluding oxygen)

The XPS technique also allows the chemical bonds present to be studied. In Figure 7 the spectra of the signal O 1s have been superposed versus depth (sputter time). To be noted is a displacement of the spectra towards higher binding energies[4], as the distance from the surface increases, which indicates a decrease in the Fe–O bonds, which are more abundant in the surface area, and an increase in the phosphorus bonds (Fe–P–O and P–O–P) with depth.

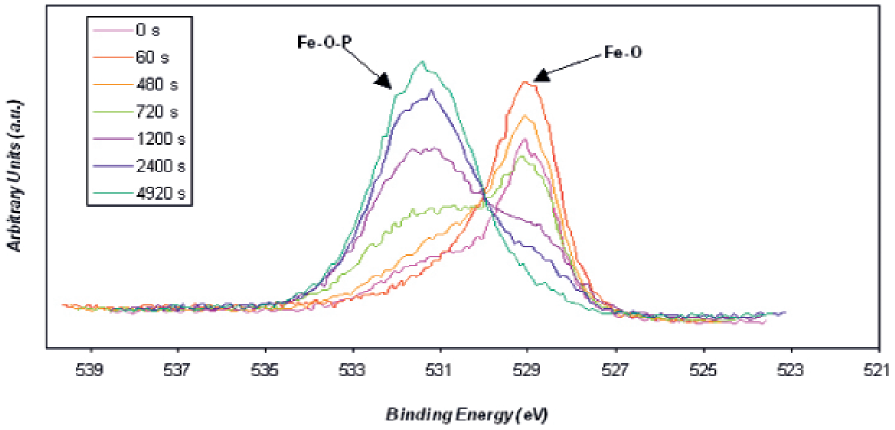

Figure 7. XPS Analysis in the region of binding energy corresponding to O 1s for the glaze Ap

The oxidation states of the iron ions can be analysed in the same way. Figure 8 shows the evolution of the Fe 2p spectrum with sputter time. At the surface, at sputter time t=0, the spectrum corresponds to the binding energy of Fe^{3+}, which is why all iron would be in this oxidation state and would be responsible for the iron oxide crystallisations like hematite, which produce the metallic effect[5]. However, further inwards, the system evolves towards a mixture of Fe^{2+} and Fe^{3+}, with a decrease in intensity. This suggests that the initial glaze contains an equilibrium between both oxidation states, and that at greater depths, the iron concentration is smaller and forms part of the glassy structure.

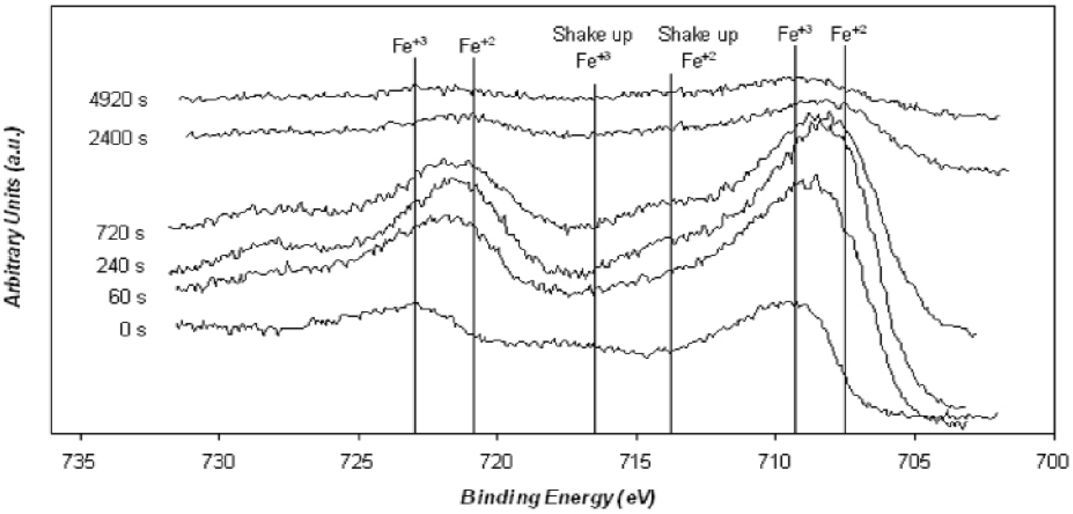

Figure 8. XPS analysis in the binding energy region corresponding to Fe 2p.

On the other hand, the attacked surface of the pieces was observed by SEM. Figure 9 shows the attacked glaze surface, and Figure 10 the profile, where the chemical attack is observed mainly to affect the intermediate glaze area **b** and the area occupied by the acicular crystallisations, in which the surrounding glaze has disappeared, the rest of the glazed area remaining unaltered. The chemical attack penetrates into area **b** presumably through irregularities in the surface layer or cracks in the glaze, advancing through the inside of layer **b**, attacking it completely, as it does layer **c**, and penetrating some distance into layer **d**.

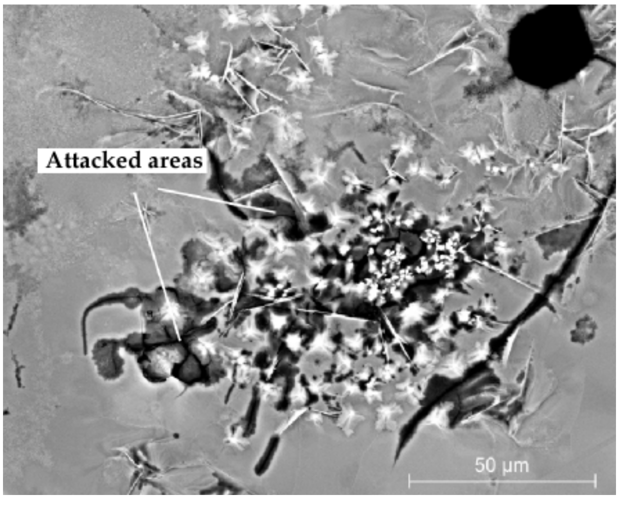

Figure 9. Surface of glaze Ap attacked with HCl

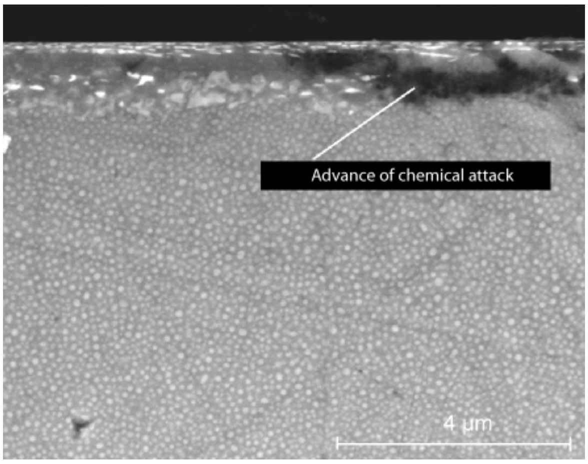

Figure 10. Profile of glaze Ap attacked with HCl

Figure 11 shows the attack undergone by glaze **Ap** with KOH. Wide areas of the surface have been attacked, making the microstructure stand out, while the unattacked areas remain smoother. The attack is almost complete, as more clearly evidenced in the profile shown in Figure 12, where layers **a**, **b**, and **c** have disappeared, though it seems that the chemical attack has been halted at layer **d** with phase separation.

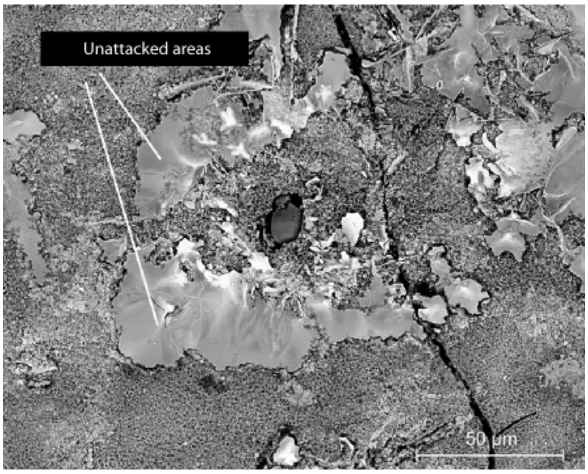

Figure 11. Surface of glaze Ap attacked with KOH

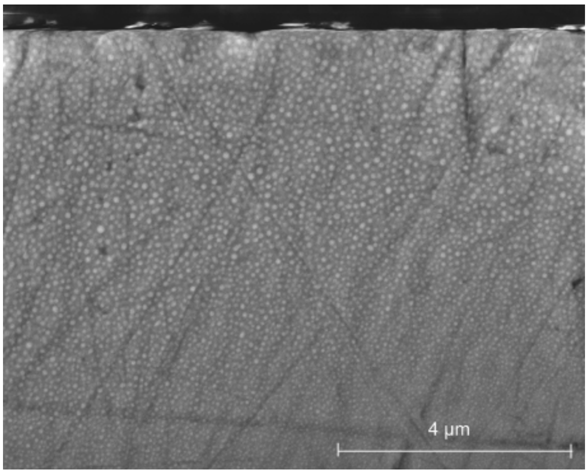

Figure 12. Profile of glaze Ap attacked with KOH

Comparison of the profile in Figure 12 with the overall analysis of the surface attacked with KOH, plotted in Figure 13, in which the drastic decrease in the peak corresponding to iron can be observed, confirms the disappearance from the surface layer of hematite devitrification.

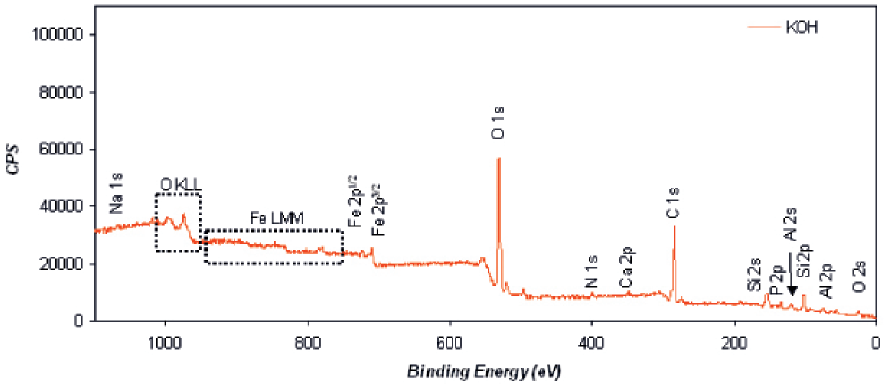

Figure 13. XPS overall analysis of the surface attacked with KOH

Finally, Figure 14 displays the XPS composition profile of the glaze attacked with KOH. It shows that layer **a**, rich in oxygen and iron, which was initially observed in the standard glaze, does not appear either; nor does the initial concentration gradient corresponding to layer **b**, which corroborates the indiscriminate attack of KOH in practically the entire glaze surface.

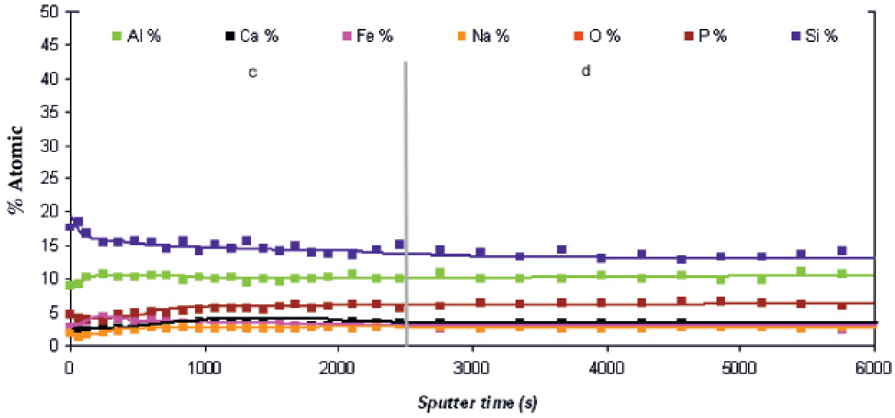

Figure 14. Profile of the glaze composition attacked with KOH

In view of the preceding tests, it appears that the main chemical acid attack occurs by the dissolution of the glassy phase in the top layers, which is why the study of the residual glaze phase after devitrification is fundamental, with a view to improving the chemical stability of the ensemble.

5. DEVELOPMENT OF NEW GLAZE COMPOSITIONS

The objective of this part of the study was, therefore, to obtain frit compositions that, on the one hand, gave rise to glazes in which the residual glassy phase was not attacked by the chemical agents and which, on the other hand, appreciably reduced the coefficient of expansion of the glassy ensemble. The foregoing data was used to formulate phosphorus glazes as a function of the different ions that make up the structure of the glaze, and of the stability of the resulting chemical bond[6]. Frit compositions with very low coefficients of expansion were obtained by modification of the mole quantities of the alkaline and alkaline-earths element on a fixed SiO_2–Al_2O_3 base. The studied range of compositions is given in Table 3:

SiO_2	Al_2O_3	R_2O	RO
50 – 75%	10 – 30%	0 – 15%	0 – 15%

Table 3. Studied range of compositions

The various glazes were formulated from these frits and metallic pigments. It was verified that the nature of the frit had a relative influence on the appearance and colour of the glazes. Table 4 presents the data on the gloss and impairment of appearance (according to Equation 1) for six frits, referenced **F1** to **F6**:

Frit ref.	20º	60º	85º	Appearance	$\Delta\Psi_{HCl}$	$\Delta\Psi_{KOH}$
F1	15.5	65.1	64.9	Strongly metallised, satin gold	6.1	9.8
F2	102.0	190.0	88.0	Very glossy, dark metallised	24.9	13.8
F3	45.5	131.6	79.6	Glossy, bluish, highly metallised,	24.9	5.5
F4	32.6	101.4	71.4	Semi-glossy, steel metallised,	22.9	35.2
F5	14.2	58.7	74.8	Dark, matt, little metallised,	24.2	27.6
F6	47.0	141.3	59.5	Glossy, bluish metallised,	47.0	41.6

Table 4. Variation of gloss with the frit used

A gloss peak is observed at 60º, typical of a metallic appearance, except in the case of frit **F1**, since this was a satin glaze, and in the case of **F6**, which had a little metallic appearance. Frit **F1** was selected as the best, since it enabled the development of glazes with a very good metallic appearance, moderate chemical attackability, and a very low frit coefficient of expansion: $21 \cdot 10^{-7}$ ºC^{-1}.

5.1. IMPROVEMENT OF THE CHEMICAL RESISTANCE OF THE GLAZES

This part of the project was conducted paying special attention to the porcelain tile glazes, in which the improvement in chemical resistance was most needed.

Metallised glaze formulations were developed that included various quantities of frit **Fa**, together with various metallic pigments, **P1**, **P2**, and **P3**. Table 5 details the results for two of the new porcelain tile glazes, **Ap1** and **Ap2**, compared with those of the previous glazes, **R** and **Ap**.

Glaze	Reagents	Classification according to standard	ΔE_q	$\Delta\Theta$	$\Delta\Psi$
R	Hydrochloric acid 18%	GHC	3.22	29.9	30.1
	Potassium hydroxide 100 g/l	GHC	32.89	94.7	100.3
Ap	Hydrochloric acid 18%	GHB	0.34	4.97	4.98
	Potassium hydroxide 100 g/l	GHC	7.79	35.5	36.3
A1p	Hydrochloric acid 18%	GHB	0.97	3.63	3.76
	Potassium hydroxide 100 g/l	GHA	0.64	3.23	3.30
A2p	Hydrochloric acid 18%	GHA	1.10	3.07	3.26
	Potassium hydroxide 100 g/l	GHA	1.63	1.57	2.26

Table 5. Chemical resistance of newly formulated glazes

Figure 15 shows the surface of glaze **A1p**. It may be observed that it is a much more homogeneous glaze than Ap, mainly made up of acicular crystallisations and other glossier ones. Figure 16 displays the profile of this glaze in which, unlike in the previous glaze **Ap**, the transition of layers **b** and **c** is subtler, and in layer **d** the points that are noted appear to correspond to crystallisations, and not to phase separation, though owing to their small sizes their nature could not be determined.

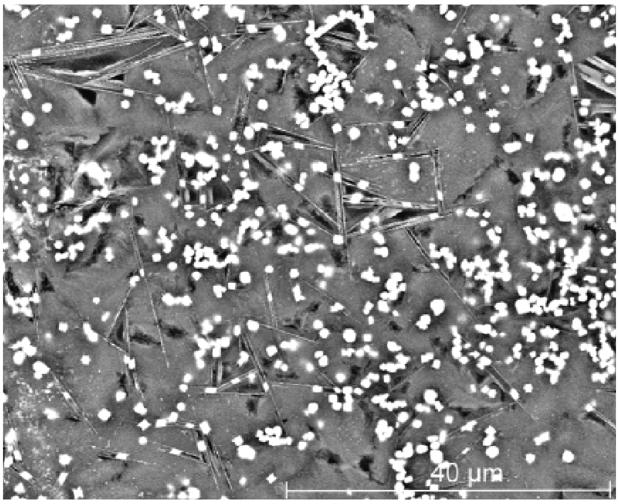

Figure 15. Surface of glaze A1p

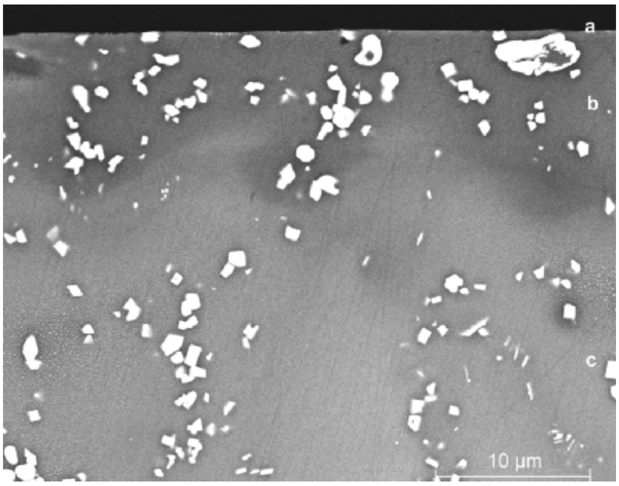

Figure 16. Profile of glaze A1p

Figure 17 shows the surface of piece **A1p** attacked with 18% HCl, in which a more defined microstructure is observed, owing to the chemical attack. This attack apparently begins around the acicular crystallisations and progresses towards the interior of the glaze, as may be observed in Figure 18.

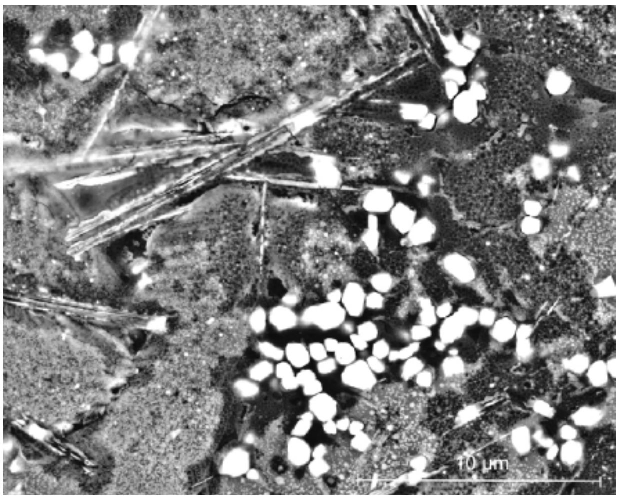

Figure 17. Surface of the A1p glaze attacked with HCl.

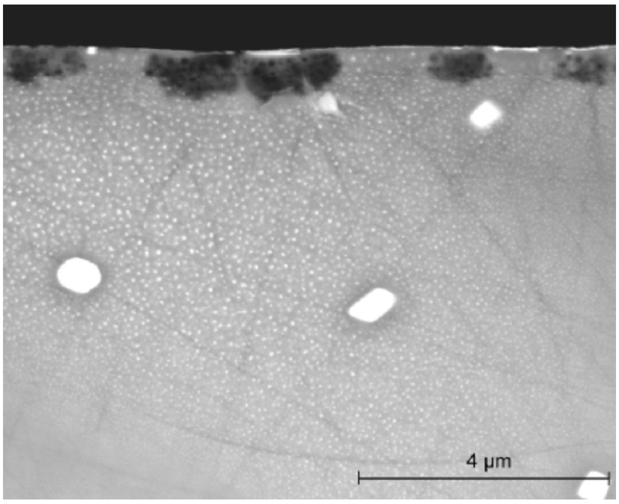

Figure 18. Profile of the A1p glaze attacked with 18% HCl

Figure 19 presents the EDX analysis of the profile of layer **b** attacked by HCl, in which an important increase in the silicon concentration and decrease in the remaining glaze constituents compared with those of the initial composition are to be noted, as a result of the dissolution of part of the glaze.

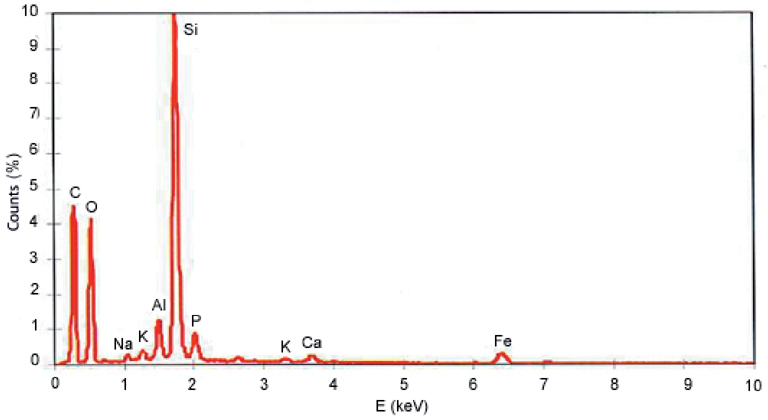

Figure 19. EDX analysis of the area attacked with 18% HCl observed in the cross-section of glaze Ap1

Figure 20 presents the XPS profiles of the compositions, which evidence a slight increase in the silicon concentration at the surface and decrease in iron as a result of the dissolution of part of the crystallisations. There is no important difference compared with the unattacked sample, since the XPS test provides an average of the surface, and the attacked areas correspond to a very small fraction of the entire surface.

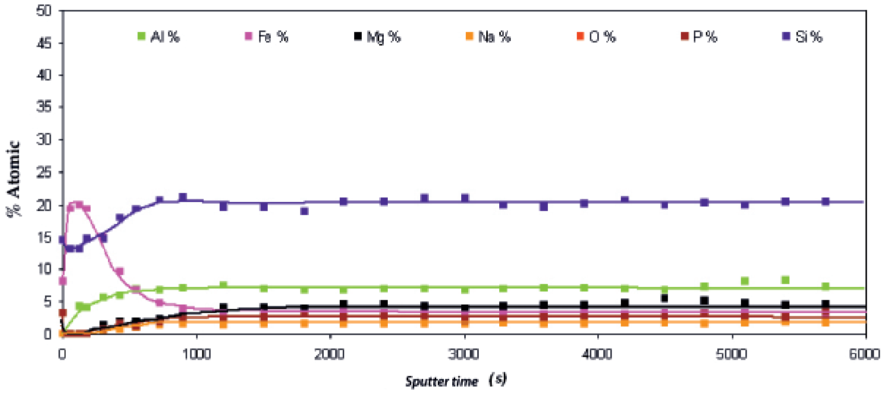

Figure 20. Profile of compositions of the A1p sample attacked with 18% HCl

In the case of KOH, examined by SEM, some darker areas are observed than those that are only detected at 10 kV, so that the attack just seems to be superficial, while large smooth areas also remain in which no type of attack seems to have occurred. Figure 21 shows the attack undergone by the surface, where only the residual glass in the devitrification areas of the acicular crystals is attacked. Figure 22 presents the profile of the glaze, with one of the small areas in which chemical attack has been occurred by KOH.

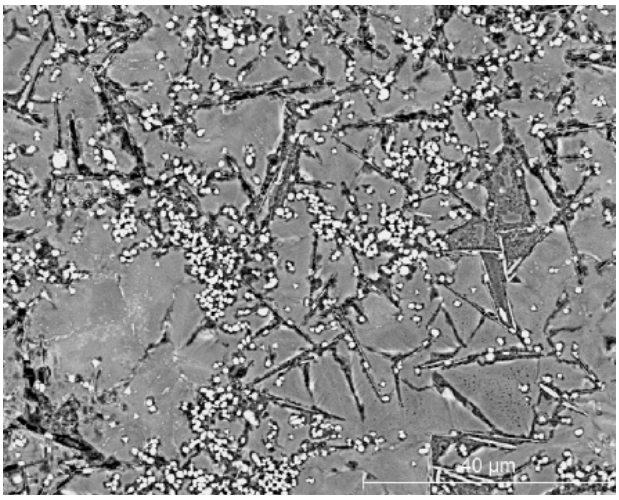

Figure 21. Surface of the A1p glaze attacked with KOH

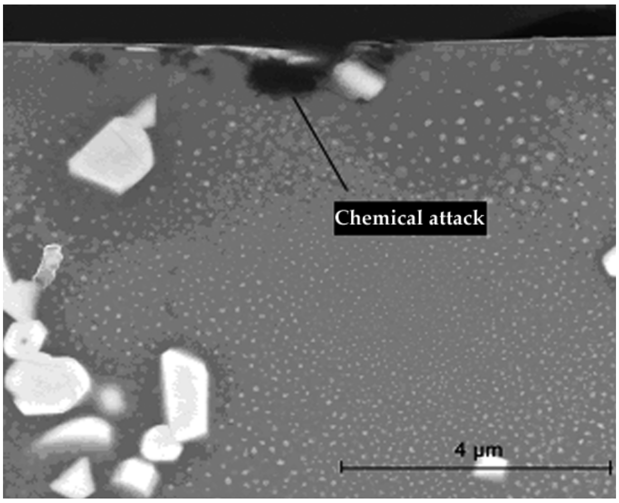

Figure 22. Cross-section of the A1p glaze attacked with KOH

The level of attack with KOH is minimum, hardly being appreciable by the naked eye, which explains its classification as GHA.

5.2. IMPROVEMENT OF THE FIT WITH THE BODY

The introduction of special frits in the formulation of metallised glazes allows a very important reduction in the coefficient of the glazes. Frit **Fa** was selected out of the studied frits; it had an expansion coefficient of $\alpha_{50\text{-}300} = 21{\cdot}10^{-7}{}^{\circ}C^{-1}$ that was especially appropriate since, as commented previously, it did not adversely affect the metallic appearance or the quality of the resulting surface, while contributing, moreover, to the improvement of chemical resistance. Table 6 presents the data corresponding to the effect of the modification of two glazes with the introduction of the frit: a porous single-fire glaze (**B** series) and a porcelain tile glaze with a very good metallic appearance, but with a very high coefficient of expansion (**C** series). In both cases, an important decrease in the coefficient is obtained, which allows stresses to be minimised, and avoids needing to use too vigorous corrective backgrounds that would create residual stresses.

Glaze ref.	Frit F % in the glaze	α_{50-300}
B	0.0	151.0
B1m	11.2	123.6
B2m	24.7	51.8
Cp	0.0	168.3
C1p	13.8	153.6
C2p	37.6	114.6

Table 6. Variation of the thermal expansion of a porous single-fire glaze with the corrective frit Fa %

6. CONCLUSIONS

The chemical attack mechanism on metallised glazes of the system P–Al–Fe has been studied. It was found that the acid attack appeared mainly to affect the residual glaze that remained in the top layers after the crystallisation of magnetite, whereas the alkaline attack was much more widespread.

A series of metallised glazes with very good fit to the body have been obtained, by using special frits with very low expansion. These glazes are especially interesting for their use in the manufacture of ceramic wall tiles, since they eliminate the problems of crazing, and the incorporation of very corrective engobes or backgrounds is not necessary, so that internal stresses and curvature problems are reduced, and large-sized tiles can be manufactured.

Metallised glaze formulations have been developed with much greater chemical resistance, by the use of the special frits mentioned previously and new metallic pigments. The glazes exhibit a much more homogeneous appearance, maintaining the metallic gloss properties, without surface defects, which makes them appropriate for use in the manufacture of ceramic floor and wall tiles. The results of this research are currently protected by a patent application.

The X-ray photoelectron spectroscopy (XPS) technique has been used with the collaboration of I.T.C. to characterise the glazes, and it has proven to be a very effective method for the study of surface effects such as metallised glazes, in which the variation of the composition and bonds is vital for appropriate constraint of the glaze reaction mechanisms.

REFERENCES

[1] RINCÓN, J.M.; ROMERO, M.. Reflective iridescent / aventurine surface glass – ceramic obtanined from mica and mineral wastes. En: Glass–Ceramic Materials. Fundamentals and Applications.Mucchi Editore, 153-164, (1997).

[2] HUNTER, R.; HAROLD, R.;. The measurement of apperarance. 2ª Edición (1997).

[3] MINFRAY, C. et al. A multi-technique approach of tribofilm characterisation. En: Thin Solid Films 447 –448 (2004) 272–277

[4] BROS, R.K.; ARENS, C.M.; YU, X.; DAY, E.. An XPS study or iron phosphate glasses. En: Physics and Chemistry of Glasses. Vol. 35 Nº3, (Junio 1994).

[5] OSAKA, A.; IKEDA, K.; MIURA, Y.; NAMBA, T. y TAKADA, J.. Preparation and magnetic properties of Ca-P-Si-Fe-O glass-ceramics.

[6] BURLING, L. Novel phosphate glasses for bone regeneration applications. Thesis submitted to the University of Nottingham. (Sep 2005).